Published in final edited form as:
Biochemistry. 2013 March 5; 52(9): 1622–1630. doi:10.1021/bi3014467.

Structural Dynamics of Actin during Active Interaction with Myosin Depends on the Isoform of the Essential Light Chain

Ewa Prochniewicz, **Piyali Guhathakurta**, and **David D. Thomas***
Department of Biochemistry, Molecular Biology and Biophysics, University of Minnesota, Minneapolis, MN 55455

Abstract

We have used time-resolved phosphorescence anisotropy (TPA) to investigate the effects of essential light chain (ELC) isoforms (A1 and A2) on the interaction of skeletal muscle myosin with actin, in order to relate structural dynamics to previously reported functional effects. Actin was labeled with a phosphorescent probe at C374, and the myosin head (S1) was separated into isoenzymes S1A1 and S1A2 by ion-exchange chromatography. As previously reported, S1A1 exhibited substantially lower ATPase activity at saturating actin but substantially higher apparent actin affinity, resulting in higher catalytic efficiency. In the absence of ATP, each isoenzyme increased actin's final anisotropy cooperatively and to a similar extent, indicating similar restriction of the amplitude of intrafilament rotational motions in the strong-binding (*S*) state of actomyosin. In contrast, in the presence of saturating ATP, S1A1 increased actin anisotropy much more than S1A2 and with greater cooperativity, indicating that S1A1 was more effective in restricting actin dynamics during the active interaction of actin and myosin. We conclude that during the active interaction of actin and ATP with myosin, S1A1 is more effective at stabilizing the *S* state (probably the force-generating state) of actomyosin, while S1A2 tends to stabilize the weak-binding (non-force-generating) *W* state. When a mixture of isoenzymes is present, S1A1 is dominant in its effects on actin dynamics. We conclude that ELC of skeletal muscle myosin modulates strong-to-weak structural transitions during the actomyosin ATPase cycle in an isoform-dependent manner, with significant implications for the contractile function of actomyosin.

Muscle contraction results from cyclic interactions of myosin and actin, fueled by ATP hydrolysis. During this interaction, the actomyosin complex undergoes transitions between weakly and strongly bound structural states, which are influenced by the biochemical state, as defined by the form of the myosin-bound nucleotide. A.M.ATP and A.M.ADP.P_i tend to populate weak-binding (non-force-generating) structural states of actomyosin (designated *W* below), producing a K_d that is more than 100-fold higher than observed for A.M.ADP and A.M, which populate mostly strong-binding (force-generating) structural states (designated *S* below). The weak-to-strong (*W*-to-*S*) structural transition of actomyosin involves structural changes in both myosin and actin.(1–7)

The myosin heavy chain starts with the N-terminal catalytic ("motor") domain, which contains sites for both actin and nucleotide binding, and extends into the light-chain ("lever arm") domain, which contains binding sites ("IQ domains") for one essential light chain (ELC) and one regulatory light chain (RLC). Rabbit skeletal muscle myosin has two ELC isoforms, originally named alkali 1 (A1) and alkali 2 (A2),(8) and one RLC isoform. The present study deals with the chymotryptic subfragment 1 (S1) (Figure 1), which is truncated within the second IQ domain, lacks RLC, and is the minimal myosin head required for actin-

Corresponding author: ddt@umn.edu. Phone: (612) 625-0957.

activated ATPase and motility.(9, 10) The two ELC isoforms differ by 41 additional N-terminal residues in A1, along with several variations in the 42–52 sequence; the remaining 141 residues are identical.(11) Chymotryptic S1 can be chromatographically separated into two isoenzymes, S1A1 and S1A2.(12) The ELC isoform does not affect the ATPase kinetics of S1 in the absence of actin(13) but has significant effects in the presence of actin, resulting in much higher catalytic efficiency for the A1 isoform.(14) Since this difference in catalytic efficiency in solution is prominent at low ionic strength but not at ionic strength approaching physiological, it has been suggested that the light chain isoforms may not have physiologically relevant differences.(14, 15)

Fluorescence microscopy and optical trapping have been used to explore the roles of ELC isoforms at the single-molecule level,(16) showing that removal of ELC from skeletal muscle myosin significantly inhibits the *in vitro* motility of actin and actomyosin force,(17) while retaining ~50% of ATPase activity.(18) When skeletal muscle myosin was selectively enriched in A2, the rate of *in vitro* actin motility was substantially higher.(19) The unloaded shortening velocities of skeletal muscle fibers of rat and rabbit were found to increase proportionally to the content of A2. (20–22) These consistent results on purified proteins and muscle fibers suggested that myosin's ELCs are involved in regulation of shortening velocity in muscle.

Functional differences between the two isoenzymes are probably due to the presence of the N-terminal extension of A1. The synthetic N-terminal peptide of A1 showed substantial effects on the ATPase activity and contractility of cardiac muscle fibers and myofibrils.(16, 23) The N-terminal extension of A1 does not appear in any crystal structure, but modeling of S1A1 into the rigor (strong-binding) acto-S1 complex led to a proposal that the positively charged residues at the N-terminus of A1 interact with negatively charged residues of subdomain 1 on a different actin protomer (Figure 1).(24, 25) This proposal is consistent with cryoelectron microscopy.(26) The involvement of the N-terminal residues of A1 in binding S1A1 to actin is supported by results from mutagenesis, crosslinking, and NMR (27–29)

We hypothesize that functional differences associated with different ELC isoforms involve A1-mediated effects on the structural states of both actin and myosin in the actomyosin ATPase cycle. To test this hypothesis, we detected the microsecond rotational dynamics of actin during interaction with S1A1 and S1A2 in the absence and presence of saturating ATP, using time-resolved phosphorescence anisotropy (TPA). TPA has been used previously to detect changes in actin filament rotational dynamics, associated with structural changes in actin itself or actin-bound myosin (2, 30–37), showing that this method provides a direct and sensitive measure of structural transitions in the acto-S1 complex. Our results in the present study showed that S1-induced changes in actin dynamics, particularly in the presence of saturating ATP, depend on the isoenzyme, with S1A1 being much more effective than S1A2 in restricting the amplitude of actin's intrafilament rotational motions.

METHODS

Protein Preparations

Actin was prepared from rabbit skeletal muscle as previously described(2) by extracting acetone powder in cold water, polymerizing with 30 mM KCl for 1 hr at room temperature, and centrifuging for 30 min at 350,000xg. The pellet was suspended in G-Mg buffer (5 mM Tris, 0.5 mM ATP, 0.2 mM $MgCl_2$, pH 7.5); pH values of all buffers were adjusted at 25 °C.

S1 was obtained by α-chymotryptic digestion of rabbit skeletal muscle myosin and separated into two isoenzymes, S1A1 and S1A2, by ion exchange chromatography on a

Trisacryl column using a gradient of 0–200 mM KCl in 10 mM imidazole (pH 7.0).(38) Fractions containing each isoenzyme were concentrated in Amicon concentrators, exhaustively dialyzed into 10 mM Tris (pH 7.5) and frozen in liquid N_2 in the presence of 150 mM sucrose used as a cryoprotectant. Before each experiment, the isoenzymes were thawed and dialyzed into Mg-F buffer (3 mM $MgCl_2$, 10 mM Tris, pH 7.5).

Labeling actin at Cys 374 with erythrosin iodoacetamide (ErIA, AnaSpec) was performed as described previously.(2) Actin (48 μM) was polymerized with 2 mM $MgCl_2$ in 20 mM Tris (pH 7.5), ErIA (freshly dissolved in DMF), was added at a concentration of 480 μM, and the sample was incubated overnight at 4° C. Labeling was terminated by adding 10 mM DTT, actin was ultracentrifuged 30 min at 350,000xg, pellets were suspended in G-Mg-buffer, clarified by 10 min centrifugation at 300,000xg, and actin was polymerized for 30 min at 25°C by adding 3 mM $MgCl_2$. After 30 min ultracentrifugation at 350,000xg, pellets were suspended in Mg-F-buffer containing 0.2 mM ATP, and the labeled F-actin was immediately stabilized against depolymerization and denaturation by adding 1 molar equivalent of phalloidin. The stabilization of actin by phalloidin was critical, since multiple control experiments showed that at pH >7.0 phalloidin-free ErIA-actin filaments are unstable and show time-dependent depolymerization and/or denaturation. The extent of labeling (mol dye/mol actin), determined by measuring absorbance of labeled actin at 538 nm and assuming molar extinction coefficient of 83000(39), was 1.0 ± 0.1 (mean ± SD, n=10). The concentration of S1 was determined by measuring absorbance at 280 nm, assuming molar extinction coefficients of 0.75 mg mL^{-1} cm^{-1} and the following molecular weights: S1 110 000, S1A1 112 000, S1A2 106 000.(27) The concentration of labeled actin was measured by the Bradford protein assay (BioRad) using unlabeled actin of known concentration as a standard.

TPA Experiments

Phalloidin-stabilized ErIA-F-actin was diluted in Mg-F-buffer to 1.0 μM, and acto-S1 complexes were formed by adding 0.1 – 6 μM S1 (also in Mg-F buffer), as indicated below. To maximize phosphorescence signals and prevent photobleaching of the dye, oxygen was removed from the sample by 5-min incubation with glucose oxidase (55 μg/ml), catalase (36 μg/ml), and glucose (45 μg/ml). Phosphorescence was measured at 25°C as described previously.(2) Actin-bound ErIA was excited with a vertically polarized 1.2-ns pulse from a FDSS 532-150 laser (CryLas) at 532 nm, operating at a repetition rate of 100 Hz. Phosphorescence emission was selected by a 670 nm glass cutoff filter (Corion), detected by a photomultiplier (R928, Hamamatsu), and digitized by a transient digitizer (CompuScope 14100, GaGe) at a time resolution of 1 μs/channel. The time-resolved phosphorescence anisotropy decay was calculated as $r(t) = [I_v(t) - GI_h(t)]/[I_v(t) + 2GI_h(t)]$, where $I_v(t)$ and $I_h(t)$ are vertically and horizontally polarized components of the emission signal, detected at 90° with a single detector and a Polaroid sheet polarizer that alternated between the two orientations every 500 laser pulses. G is an instrumental correction factor, determined by performing the measurement with horizontally polarized excitation, for which the corrected anisotropy value is set to zero.

The time-resolved anisotropy decays of free actin and rigor complexes (no ATP) with S1 were obtained by recording 20 cycles of 1000 pulses (500 in each orientation of the polarizer), corresponding to a total acquisition time of about 4 minutes. To analyze complexes in the presence of saturating ATP, 3 mM ATP was added directly to the cuvette containing acto-S1 (0.3 – 4 μM S1A1 or 0.3–6 μM S1A2), the sample was gently mixed, and 30 s later 3 cycles of 1000 pulses were recorded, as in our previous experiments.(2, 34) The 3 cycles were repeated four times, for a total time of data acquisition of 3 min. Data was only retained if these four data sets gave equivalent results, indicating that ATP remained saturating.

TPA Data Analysis

Final anisotropy (r_∞) was defined as the average value of r in the time window from 400 to 500 μs, which has been shown previously to provide the most sensitive and precise measurement of actin's microsecond rotational dynamics.(2) The effects of bound S1 on the final anisotropy of actin was analyzed using the linear-lattice model as in our previous work.(2, 30) This model assumes that perturbation of one protomer in an actin filament affects a segment containing N protomers:

$$r = r_{max} - (r_{max} - r_{actin})\,(1-x)^N \quad \text{Eq. 1}$$

where r_{actin} and r_{max} are the limiting values of anisotropy at 0 and saturating concentrations of S1, and x = [S1]/[actin] binding density. The adjustable parameters in the fit were r_{max} and N.

Functional Interaction of S1 Isoenzymes with Actin

Biochemical assays were performed using the same samples as prepared for the spectroscopic experiments. The affinity of S1 for actin in saturating ATP was measured at 25°C in Mg-F-buffer containing 3 mM ATP.(34) K_d was determined by fitting the data to

$$S1_b/S1_t = [A]/([A]+K_d) \quad \text{Eq. 2}$$

using Origin 8.0, where $S1_b/S1_t$ is the fraction of S1 bound to actin, and [A] is the concentration of free actin.

The fraction of actin containing bound S1, under conditions of TPA measurements where S1 was at molar excess over actin, was calculated from the quadratic binding equation:

$$A_b/A_t = \{(S_t + A_t + K_d) - [(S_t + A_t + K_d)^2 - 4A_tS_t]^{0.5}\}/2A_t, \quad \text{Eq. 3}$$

where A_b is the concentration of actin occupied by S1, K_d is the dissociation constant determined in the sedimentation assay (Eq. 2), and the total concentrations of S1 and actin are S_t and A_t, respectively.

Actin-activated ATPase activity was measured at 25°C in Mg-F-buffer containing 3 mM ATP at constant concentration of S1 (0.2 μM) and increasing concentrations of ErIA-actin. P_i was determined by the malachite green method.(40) V_{max} and K_{ATPase} of acto-S1 ATPase were determined by fitting the data to

$$V = V_{max}[A]/([A]+K_{ATPase}) \quad \text{Eq. 4}$$

using Origin 8.0. Uncertainties of K_d, V_{max} and K_{ATPase} were determined from statistical analysis of the fits.

RESULTS

Enzymatic Properties of S1 Isoenzymes

In the absence of actin, the high-salt ATPase activities of S1A1 and S1A2 were essentially the same: K-ATPase was 11.6±1.2 s^{-1} and 12.0±0.1 s^{-1} and Ca/K-ATPase was 1.2±0.1 s^{-1} and 1.4±0.2 s^{-1}, respectively, confirming previous reports that the isoform of ELC does not affect enzymatic properties of isolated S1.(12)

In contrast, the ELC isoform had significant effects on the functional interaction of S1 with ErIA-actin, particularly at low ionic strength, i.e., in the absence of KCl. The catalytic efficiency (V_{max}/K_{ATPase}) of acto-S1A1 was about 3 times that of acto-S1A2 (Table 1, *V*Figure 2A). This difference arises from isoenzyme-dependent values of both $_{max}$ and K_{ATPase}, as previously reported for unlabeled actin.(14) Control experiments showed that the difference in the enzymatic activities of the two isoenzymes, particularly in V_{max}, significantly decreased when the ATPase measurements were performed at a constant concentration of actin and increasing concentrations of each isoenzyme (data not shown). This result is also consistent with previous studies proposing that the rate of product release is the same for both isoenzymes, but for S1A1 other processes become rate-limiting.(14)

Cosedimentation assays in the presence of saturating ATP showed that the actin affinity of S1A1 was about two-fold higher than that of S1A2 (Figure 2B). This difference in K_d is less pronounced than the 5-fold effect previously reported for unlabeled actin,(41) probably due to the enhancing effect of the ErIA label on actin affinity for S1.(2) Increasing ionic strength to 25 mM KCl substantially decreased isoenzyme differences in actin interaction (Table 1), confirming previous reports on unlabeled actin.(14, 41)

Effects of S1 Isoenzymes on Actin Dynamics in the Absence of ATP

Cosedimentation and pyrene fluorescence showed that both isoenzymes bind actin stoichiometrically with sub-micromolar affinity.(37) TPA decays show that binding of saturating concentrations of S1A1 or S1A2 results in a substantial increase in the final anisotropy, indicating that both isoenzymes decrease the amplitude of actin's intrafilament motions (Figure 3A). Binding of each isoenzyme increased actin's final anisotropy nonlinearly, indicating cooperativity (i.e., N > 1 in Eq. 1) in restricting the amplitude of microsecond intrafilament motions (Figure 3B). Over the entire range of binding, S1A1 was more effective in increasing actin anisotropy. A t-test (α=0.05) performed for final anisotropy values at 0.25, 0.5 and 1 mol S1 bound per mol of actin showed that the difference in the effects of isoenzymes is statistically significant: the calculated values of t (4.44, 9.93 and 3.46) were higher than corresponding values of t_c (2.78, 2.57 and 2.45). Fitting the anisotropy increase to the linear lattice model (Eq. 1) showed that the final anisotropy at saturation (r_{max}) and the extent of cooperativity (N) were higher in the presence of S1A1 (r_{max} = 0.092 ± 0.002, N = 4.9 ± 0.6) than S1A2 (r_{max} = 0.081 ± 0.003, N = 3.5 ± 0.8), suggesting that the amino terminal extension of A1 enhances the restricting effect of strongly bound myosin heads on actin's intrafilament motions.

Effects of S1 Isoenzymes on Actin Dynamics in the Presence of Saturating ATP

At 3 mM ATP, the TPA decay of actin was intermediate between that of free and strongly bound (no ATP) actin, even when compared at the same fraction (0.4) of bound S1 (Figure 4A). This intermediate state of actin dynamics in the presence of ATP was previously observed with unseparated S1.(2) (34) The effects of the individual isoenzymes are shown in (Figure 4B). For each concentration of added isoenzyme (0.3 – 4 μM for S1A1, 0.5 – 6 μM for S1A2), the molar ratio of bound S1 per actin protomer (horizontal axis of Figure 4B) was calculated (Eq. 3) using K_d values from Table 1.

Actin dynamics in saturating ATP was substantially dependent on the ELC isoform (Figure 4B), much more than in the absence of ATP (Figure 3B). For S1A2, final anisotropy increased linearly with the extent of binding, and the maximum observed increase was much less than observed for S1A1 (Figure 4B). For S1A1, the effect was biphasic: at very low occupancy (≤ 0.05), anisotropy was not affected, but as binding increased, the anisotropy showed a substantial nonlinear increase. At 0.45 moles of S1A1/mol actin (the maximum achieved in this study) the final anisotropy was about 2.5 times greater than that of free

actin. This increase of final anisotropy was fitted by the linear lattice model, with r_{max} = 0.075 ± 0.006 and N = 4.4 ± 1.1, indicating that 4–5 actin protomers were affected for every S1A1 bound. Thus, while S1A2 had very little effect on actin and showed no cooperativity, S1A1 had nearly the same effect and cooperativity as in rigor, when compared at the same binding ratio (Figure 3B).

To confirm that ATP was not exhausted during TPA measurements, each data acquisition was followed by addition of 0.1 M KCl to the sample. If ATP were exhausted and strongly bound acto-S1 formed, addition of KCl would have no effect on anisotropy, but if saturating ATP were still present, the increased ionic strength would dissociate all S1 and the final anisotropy would decrease to the level of free actin. We found that complete dissociation of acto-S1 took place: addition of KCl decreased the final anisotropy to 0.025±0.006, which was essentially the same as that of free actin in the same conditions, 0.029± 0.003. This shows that ATP was saturating during TPA data acquisition.

The possibility that the TPA data are affected by aggregation of actin was excluded by observation of acto-S1 complexes with a fluorescence microscope (data not shown). Phalloidin-rhodamine-labeled filaments of unlabeled or ErIA-labeled actin in the presence of S1A1 (added up to total concentration of 4 μM, corresponding to fraction bound of 0.45) and ATP had essentially the same appearance as filaments of free phalloidin-rhodamine actin. Thus the observed changes in anisotropy in Figure 4 represent changes in the internal dynamics of actin filaments.

Effects of a Mixture of Isoenzymes

To determine whether the two isoenzymes, when added together, affect actin dynamics independently, we performed similar experiments as in (Figure 4), using a 2:1 mixture of S1A1 and S1A2, thus mimicking the native composition of rabbit psoas muscle myosin(42), and we compared the result in Figure 5 with a liner combination of data from S1A1 and S1A2 (from Figure 4). The final anisotropy increased linearly with isoenzymes mixture (Figure 5), as in the previous report on unseparated S1.(2) However, the data (open diamonds) deviated from the calculation (closed diamonds) at higher levels of saturation, where the observed effect was greater than calculated (Figure 5). This suggests that when both isoenzymes interact with actin, the effect of S1A1 is dominant.

Effects at Increased Ionic Strength

To test whether different effects of weakly bound S1A1 and S1A2 on actin anisotropy in the presence of saturating ATP (Figure 4) are associated with differences in biochemical interactions, we performed measurements in the presence of 25 mM KCl, where isoenzyme differences in binding affinity and actomyosin ATPase activities significantly decrease (Table 1). At 0.3 bound isoenzyme/mol actin (4 μM total), the final anisotropy of actin in the presence of S1A2, 0.032 ± 0.003 was essentially the same as that of actin alone, 0.029 ± 0.004, but the final anisotropy of actin in the presence of S1A1 was significantly higher, 0.050 ± 0.006. This suggests that the observed differences in structural effects of isoenzymes (Figure 4) are not tightly coupled to biochemical states and may be relevant for actomyosin interactions at increased ionic strength, including physiological conditions (~100–140 mM K^+).(43) Solution experiments at physiological ionic strength were not feasible, since decreased affinities of actin for myosin (K_d > 100 μM,(44)) require proteins at concentrations too high for optical measurements. Nevertheless, results of our previous studies indicate that differences in the dynamics of S1-bound actin detected at low ionic strength can be relevant to actomyosin interactions at physiological conditions. For example, in a study of oxidation effects in muscle, we found that TPA differences observed in

solution at low ionic strength (no KCl) were consistent with differences in the structural states of myosin in muscle fibers, observed at 130 mM K^+.(32, 34)

DISCUSSION

Previous studies have shown that the actin filament has a wide repertoire of functionally important intrafilament structural dynamics, tuned to the structure of its binding partners, whether they be different myosin isoforms,(30, 33) post-translationally modified myosin, (31, 34) or other actin-binding proteins.(45–48) In the present study, we have found that the effects of myosin on the structural dynamics of actin depend substantially on the isoform of myosin's ELC, especially during the actomyosin ATPase cycle. Both S1A1 and S1A2 have substantial, but significantly different, effects on the restriction of actin rotational dynamics in the strongly bound complex in the absence of ATP (Figure 3). This isoform dependence is much more pronounced in the presence of saturating ATP, which greatly reduces the effect of S1A2 on actomyosin dynamics, but only slightly reduces the effect of S1A1 (Figure 4). We conclude that during the actomyosin ATPase cycle the presence of the A1 light chain shifts the distribution of structural states of actin toward the strongly bound structural state, while the presence of the A2 light chain shifts the distribution towards the weakly bound structural state.

Actomyosin in the Absence of ATP

The different effects of S1 isoenzymes on actin dynamics are associated with the presence of the extended N-terminus in the A1 light chain. Electron microscopy, mutations, crosslinking and modeling studies have led to the proposal that the positively charged N-terminus of A1 binds to the negatively charged C-terminal region of an actin protomer that is distinct from the protomer that binds the catalytic domain (Figure 1).(16, 25–29, 49–51) This additional contact between S1 and actin could result in more restricted intrafilament motions in acto-S1A1 than in acto-S1A2. An alternative has been proposed – that the N-terminus of A1 binds to the converter region of the S1 heavy chain, (52, 53) which allosterically affects the interaction with actin. That hypothesis is not backed by direct evidence, but it is consistent with allosteric effects in Dictyostelium myosin II(54) and non-muscle myosin VI.(33)

Actomyosin in the Presence of Saturating ATP

Much more substantial differences in the effects of isoenzymes on actin's dynamics were observed in the presence of ATP (Figure 3, Figure 4), showing that the effects of light-chain isoforms depend on the structural state of the myosin head. Spectroscopic studies with probes on myosin have shown that in the presence of saturating ATP, actin-attached myosin exists in two predominant structural states: *W* (weakly bound) and *S* (strongly bound).(4, 55–59) In the *S* state, myosin heads form stereospecific contacts with actin, while in the *W* state the catalytic and light-chain domains of the myosin head show rotational disorder on the microsecond time scale.(4, 24, 55, 58, 60–64) TPA studies with probes on actin have shown that actin also has two predominant structural states, *S* and *W* (more dynamically disordered), related to the structural states of the interacting myosin head.(2, 6, 7)

Proposed Structural Model

In the present study, we interpret TPA data in terms of a simple two-state structural model (Figure 6B), which is supported by TPA data in the present and previous studies. In this model, actin structural dynamics, as indicated by the final TPA anisotropy (r_∞), is not significantly affected by myosin in the *W* state ($r_\infty = r_{actin}$) (Figure 3), and *S* is the state of actin having minimum flexibility, in which the final anisotropy is the same as in the fully saturated rigor complex ($r_\infty = r_{max,}$ determined from Figure 3 by fitting with Eq. 1). Therefore, the final anisotropy of actin interacting with myosin is given by

$$r_{\infty}=X_S\, r_{max}+(1-X_S)\, r_{actin}, \quad \text{Eq. 5}$$

where X_S is the fraction of actin protomers in the *S* state. Thus X_S can be calculated from

$$X_s=1-(r_{max}-r_{\infty})/(r_{max}-r_{actin}). \quad \text{Eq. 6}$$

Figure 6A shows plots of X_S *vs.* the fraction of actin protomers occupied by myosin in the presence of saturating ATP. A low value of X_S in acto-S1A2 indicates that the predominant structural state of acto-S1A2 is *W*, in which binding of the dynamically disordered S1A2 does not significantly restrict intrafilament motions in actin (Figure 6B, left). In contrast, X_S is substantially greater for acto-S1A1, indicating that the predominant structural state is *S* (Figure 6B, right). A likely explanation for this isoform difference is that the N-terminus of the A1 isoform of ELC tethers ELC to actin (Figure 1, Figure 6B, right), thus decreasing disorder of both actin and S1 and increasing X_S. Under our experimental conditions, as in muscle, actin is less than half saturated with S1, so the proposed binding of the catalytic domain and A1 to different protomers in the actin filament is plausible (Figure 1).

We propose that that the actin tether provided by A1 stabilizes the *S* structural state while biochemically still binding ATP. It is also possible that A1 binds to the myosin heavy chain and thus modulates myosin's structural states internally,(53) but the proposed actin tether (Figure 6B) provides a more compelling and complete explanation. This model helps explain not only the increase in X_S caused by the A1 isoform, but also the observed cooperativity, which is observed for S1A1 (curvature in Figure 6A, indicating $N > 1$ in Eq. 1), but not for S1A2 (linear dependence in Figure 6A, $N = 1$). This is consistent with the proposal that the *W* and *S* states have different interfaces with actin.(24) It is known that the strongly bound rigor complex involves the interaction of a single S1 with two actin protomers,(24, 65) as depicted in the *S* state of Figure 6B, which helps explain our previous observation that a single S1 restricts the dynamics of more than one actin protomer as detected by EPR(66) and TPA.(2) It is likely that the *W* complex involves only a single actin protomer (Figure 6B), explaining its lack of cooperativity in TPA (Figure 6A). Propagation of the S1A1-specific *S* interface beyond the directly bound actin protomers can also explain why the effect of S1A1 is dominant (Figure 5).

Significance for Muscle Physiology

The present results are consistent with previously observed changes in actin dynamics that depend on the isoform of the myosin heavy chain,(30, 33) resulting in isoform-dependent functional variation. The proposed A1-mediated shift of the structural states of actomyosin to the strongly bound *S* state is consistent with the results of mutational studies on the functional role of the N-terminus of A1 in cardiac muscle, where A1 is the only ELC. Analysis of the inhibitory effects of N-terminus removal on cardiac force led to the proposal that binding of the A1 N-terminus to actin in the presence of ATP stabilizes the post-power-stroke state of myosin and increases the population of force-generating and force-maintaining crossbridges, which were shown to be in a strongly bound structural state.(67–70) The relationship between improved contractility and stabilization of cardiac myosin in the strong-binding, force-generating state has been proposed as an important mechanism for increasing cardiac performance by a myosin-bound small molecule of therapeutic potential, with specificity for the cardiac isoform of myosin, which contains only the A1 ELC isoform.(71)

The physiological role of A1 in cardiac and skeletal muscle contractile activities was also studied using synthetic peptides corresponding to its 10–15 N-terminal amino acids.

Addition of these peptides to muscle fibers or myofibrils increased their contractility and ATPase activity (72–74, 75), but the molecular target of these peptides has not been determined.

Conclusion

The N-terminal extension in the A1 light chain of myosin ELC enhances the capacity of myosin to restrict actin's intrafilament torsional dynamics, particularly in the presence of saturating ATP. The result is a cooperative stabilization of the strong-binding structural states of both actin and myosin, providing a compelling explanation for the dependence of muscle function on the ELC isoform, with potentially profound implications for the function and regulation of striated muscle. Future studies will be needed to define the protein-protein interactions responsible for these effects.

Acknowledgments

Phosphorescence measurements were performed in the Biophysical Spectroscopy Center, University of Minnesota. We thank Octavian Cornea for assistance with manuscript preparation.

Funding: This work was supported by NIH grants to DDT (AR32961 and AR57220), and PG was supported by the Minnesota Muscle Training Grant, NIH T32 AR007612

Abbreviations

S1	myosin subfragment 1
ELC	essential light chain
TPA	Time-resolved phosphorescence anisotropy

References

1. Cooke R, Crowder MS, Thomas DD. Orientation of spin labels attached to cross-bridges in contracting muscle fibres. Nature. 1982; 300:776–778. [PubMed: 6294531]
2. Prochniewicz E, Walseth TF, Thomas DD. Structural dynamics of actin during active interaction with myosin: different effects of weakly and strongly bound myosin heads. Biochemistry. 2004; 43:10642–10652. [PubMed: 15311925]
3. Berger CL, Svensson EC, Thomas DD. Photolysis of a photolabile precursor of ATP (caged ATP) induces microsecond rotational motions of myosin heads bound to actin. Proc Natl Acad Sci U S A. 1989; 86:8753–8757. [PubMed: 2554328]
4. Baker JE, Brust-Mascher I, Ramachandran S, LaConte LE, Thomas DD. A large and distinct rotation of the myosin light chain domain occurs upon muscle contraction. Proc Natl Acad Sci U S A. 1998; 95:2944–2949. [PubMed: 9501195]
5. Holmes KC, Schroder RR, Sweeney HL, Houdusse A. The structure of the rigor complex and its implications for the power stroke. Philos Trans R Soc Lond B Biol Sci. 2004; 359:1819–1828. [PubMed: 15647158]
6. Thomas DD, Kast D, Korman VL. Site-directed spectroscopic probes of actomyosin structural dynamics. Annu Rev Biophys. 2009; 38:347–369. [PubMed: 19416073]
7. Thomas DD, Muretta JM, Colson BA, Mello R, Kast DJ. Spectroscopic probes of muscle proteins. Comprehensive Biophysics. 2012
8. Weeds AG, Lowey S. Substructure of the myosin molecule. II. The light chains of myosin. J Mol Biol. 1971; 61:701–725. [PubMed: 4257244]
9. Toyoshima YY, Kron SJ, McNally EM, Niebling KR, Toyoshima C, Spudich JA. Myosin subfragment-1 is sufficient to move actin filaments in vitro. Nature. 1987; 328:536–539. [PubMed: 2956522]

10. Waller GS, Ouyang G, Swafford J, Vibert P, Lowey S. A minimal motor domain from chicken skeletal muscle myosin. J Biol Chem. 1995; 270:15348–15352. [PubMed: 7797523]
11. Frank G, Weeds AG. The amino-acid sequence of the alkali light chains of rabbit skeletal-muscle myosin. Eur J Biochem. 1974; 44:317–334. [PubMed: 4838672]
12. Weeds AG, Taylor RS. Separation of subfragment-1 isoenzymes from rabbit skeletal muscle myosin. Nature. 1975; 257:54–56. [PubMed: 125854]
13. Taylor RS, Weeds AG. Transient-phase of ATP hydrolysis by myosin sub-fragment-1 isoenzymes. FEBS Lett. 1977; 75:55–60. [PubMed: 140068]
14. Wagner PD, Slater CS, Pope B, Weeds AG. Studies on the actin activation of myosin subfragment-1 isoezymes and the role of myosin light chains. Eur J Biochem. 1979; 99:385–394. [PubMed: 159176]
15. Pope B, Wagner PD, Weeds AG. Studies on the actomyosin ATPase and the role of the alkali light chains. Eur J Biochem. 1981; 117:201–206. [PubMed: 6455293]
16. Timson DJ. Fine tuning the myosin motor: the role of the essential light chain in striated muscle myosin. Biochimie. 2003; 85:639–645. [PubMed: 14505818]
17. VanBuren P, Waller GS, Harris DE, Trybus KM, Warshaw DM, Lowey S. The essential light chain is required for full force production by skeletal muscle myosin. Proc Natl Acad Sci U S A. 1994; 91:12403–12407. [PubMed: 7809049]
18. Lowey S, Waller GS, Trybus KM. Skeletal muscle myosin light chains are essential for physiological speeds of shortening. Nature. 1993; 365:454–456. [PubMed: 8413589]
19. Lowey S, Waller GS, Trybus KM. Function of skeletal muscle myosin heavy and light chain isoforms by an in vitro motility assay. J Biol Chem. 1993; 268:20414–20418. [PubMed: 8376398]
20. Bottinelli R, Betto R, Schiaffino S, Reggiani C. Unloaded shortening velocity and myosin heavy chain and alkali light chain isoform composition in rat skeletal muscle fibres. J Physiol. 1994; 478(Pt 2):341–349. [PubMed: 7965849]
21. Greaser ML, Moss RL, Reiser PJ. Variations in contractile properties of rabbit single muscle fibres in relation to troponin T isoforms and myosin light chains. J Physiol. 1988; 406:85–98. [PubMed: 3254423]
22. Sweeney HL. Function of the N terminus of the myosin essential light chain of vertebrate striated muscle. Biophys J. 1995; 68:112S–118S. discussion 118S–119S. [PubMed: 7787052]
23. Hernandez OM, Jones M, Guzman G, Szczesna-Cordary D. Myosin essential light chain in health and disease. Am J Physiol Heart Circ Physiol. 2007; 292:H1643–1654. [PubMed: 17142342]
24. Rayment I, Holden HM, Whittaker M, Yohn CB, Lorenz M, Holmes KC, Milligan RA. Structure of the actin-myosin complex and its implications for muscle contraction. Science. 1993; 261:58–65. [PubMed: 8316858]
25. Aydt EM, Wolff G, Morano I. Molecular modeling of the myosin-S1(A1) isoform. J Struct Biol. 2007; 159:158–163. [PubMed: 17498971]
26. Milligan RA, Whittaker M, Safer D. Molecular structure of F-actin and location of surface binding sites. Nature. 1990; 348:217–221. [PubMed: 2234090]
27. Timson DJ, Trayer HR, Trayer IP. The N-terminus of A1-type myosin essential light chains binds actin and modulates myosin motor function. Eur J Biochem. 1998; 255:654–662. [PubMed: 9738905]
28. Andreev OA, Saraswat LD, Lowey S, Slaughter C, Borejdo J. Interaction of the N-terminus of chicken skeletal essential light chain 1 with F-actin. Biochemistry. 1999; 38:2480–2485. [PubMed: 10029542]
29. Timson DJ, Trayer HR, Smith KJ, Trayer IP. Size and charge requirements for kinetic modulation and actin binding by alkali 1-type myosin essential light chains. J Biol Chem. 1999; 274:18271–18277. [PubMed: 10373429]
30. Prochniewicz E, Chin HF, Henn A, Hannemann DE, Olivares AO, Thomas DD, De La Cruz EM. Myosin isoform determines the conformational dynamics and cooperativity of actin filaments in the strongly bound actomyosin complex. J Mol Biol. 2010; 396:501–509. [PubMed: 19962990]
31. Prochniewicz E, Katayama E, Yanagida T, Thomas DD. Cooperativity in F-actin: chemical modifications of actin monomers affect the functional interactions of myosin with unmodified monomers in the same actin filament. Biophys J. 1993; 65:113–123. [PubMed: 8369420]

32. Prochniewicz E, Lowe DA, Spakowicz DJ, Higgins L, O'Conor K, Thompson LV, Ferrington DA, Thomas DD. Functional, structural, and chemical changes in myosin associated with hydrogen peroxide treatment of skeletal muscle fibers. Am J Physiol Cell Physiol. 2008; 294:C613–626. [PubMed: 18003749]
33. Prochniewicz E, Pierre A, McCullough BR, Chin HF, Cao W, Saunders LP, Thomas DD, De La Cruz EM. Actin Filament Dynamics in the Actomyosin VI Complex Is Regulated Allosterically by Calcium-Calmodulin Light Chain. J Mol Biol. 2011; 413:584–592. [PubMed: 21910998]
34. Prochniewicz E, Spakowicz D, Thomas DD. Changes in actin structural transitions associated with oxidative inhibition of muscle contraction. Biochemistry. 2008; 47:11811–11817. [PubMed: 18855423]
35. Prochniewicz E, Thomas DD. Perturbations of functional interactions with myosin induce long-range allosteric and cooperative structural changes in actin. Biochemistry. 1997; 36:12845–12853. [PubMed: 9335542]
36. Prochniewicz E, Thomas DD. Differences in structural dynamics of muscle and yeast actin accompany differences in functional interactions with myosin. Biochemistry. 1999; 38:14860–14867. [PubMed: 10555968]
37. Prochniewicz E, Thomas DD. Site-specific mutations in the myosin binding sites of actin affect structural transitions that control myosin binding. Biochemistry. 2001; 40:13933–13940. [PubMed: 11705383]
38. Trayer HR, Trayer IP. Fluorescence resonance energy transfer within the complex formed by actin and myosin subfragment 1. Comparison between weakly and strongly attached states. Biochemistry. 1988; 27:5718–5727. [PubMed: 2972314]
39. Prochniewicz E, Zhang Q, Howard EC, Thomas DD. Microsecond rotational dynamics of actin: spectroscopic detection and theoretical simulation. J Mol Biol. 1996; 255:446–457. [PubMed: 8568889]
40. Lanzetta PA, Alvarez LJ, Reinach PS, Candia OA. An improved assay for nanomole amounts of inorganic phosphate. Anal Biochem. 1979; 100:95–97. [PubMed: 161695]
41. Chalovich JM, Stein LA, Greene LE, Eisenberg E. Interaction of isozymes of myosin subfragment 1 with actin: effect of ionic strength and nucleotide. Biochemistry. 1984; 23:4885–4889. [PubMed: 6238623]
42. Weeds AG, Hall R, Spurway NC. Characterization of myosin light chains from histochemically identified fibres of rabbit psoas muscle. FEBS Lett. 1975; 49:320–324. [PubMed: 122817]
43. Godt RE, Maughan DW. On the composition of the cytosol of relaxed skeletal muscle of the frog. Am J Physiol. 1988; 254:C591–604. [PubMed: 3284380]
44. Chalovich JM, Greene LE, Eisenberg E. Crosslinked myosin subfragment 1: a stable analogue of the subfragment-1.ATP complex. Proc Natl Acad Sci U S A. 1983; 80:4909–4913. [PubMed: 6576363]
45. Prochniewicz E, Janson N, Thomas DD, De la Cruz EM. Cofilin increases the torsional flexibility and dynamics of actin filaments. J Mol Biol. 2005; 353:990–1000. [PubMed: 16213521]
46. Prochniewicz E, Henderson D, Ervasti JM, Thomas DD. Dystrophin and utrophin have distinct effects on the structural dynamics of actin. Proc Natl Acad Sci U S A. 2009; 106:7822–7827. [PubMed: 19416869]
47. Lin AY, Prochniewicz E, Henderson DM, Li B, Ervasti JM, Thomas DD. Impacts of dystrophin and utrophin domains on actin structural dynamics: implications for therapeutic design. J Mol Biol. 2012; 420:87–98. [PubMed: 22504225]
48. Galkin VE, Orlova A, Schroder GF, Egelman EH. Structural polymorphism in F-actin. Nat Struct Mol Biol. 2010; 17:1318–1323. [PubMed: 20935633]
49. Hayashibara T, Miyanishi T. Binding of the amino-terminal region of myosin alkali 1 light chain to actin and its effect on actin-myosin interaction. Biochemistry. 1994; 33:12821–12827. [PubMed: 7947687]
50. Xiao M, Tartakowski A, Andreev OA, Borejdo J. Binding of S1(A1) and S1(A2) to F-actin. Biochemistry. 1996; 35:523–530. [PubMed: 8555223]

51. Andreev OA, Borejdo J. Binding of heavy-chain and essential light-chain 1 of S1 to actin depends on the degree of saturation of F-actin filaments with S1. Biochemistry. 1995; 34:14829–14833. [PubMed: 7578092]
52. Pliszka B, Redowicz MJ, Stepkowski D. Interaction of the N-terminal part of the A1 essential light chain with the myosin heavy chain. Biochem Biophys Res Commun. 2001; 281:924–928. [PubMed: 11237749]
53. Lowey S, Saraswat LD, Liu H, Volkmann N, Hanein D. Evidence for an interaction between the SH3 domain and the N-terminal extension of the essential light chain in class II myosins. J Mol Biol. 2007; 371:902–913. [PubMed: 17597155]
54. Guhathakurta P, Prochniewicz E, Muretta JM, Titus MA, Thomas DD. Allosteric communication in Dictyostelium myosin II. J Muscle Res Cell Motil. 2012
55. Thomas DD, Cooke R. Orientation of spin-labeled myosin heads in glycerinated muscle fibers. Biophys J. 1980; 32:891–906. [PubMed: 6266539]
56. Nesmelov YE, Agafonov RV, Burr AR, Weber RT, Thomas DD. Structure and dynamics of the force-generating domain of myosin probed by multifrequency electron paramagnetic resonance. Biophys J. 2008; 95:247–256. [PubMed: 18339764]
57. Berger CL, Thomas DD. Rotational dynamics of actin-bound intermediates in the myosin ATPase cycle. Biochemistry. 1991; 30:11036–11045. [PubMed: 1657157]
58. Berger CL, Thomas DD. Rotational dynamics of actin-bound myosin heads in active myofibrils. Biochemistry. 1993; 32:3812–3821. [PubMed: 8385491]
59. Berger CL, Thomas DD. Rotational dynamics of actin-bound intermediates of the myosin adenosine triphosphatase cycle in myofibrils. Biophys J. 1994; 67:250–261. [PubMed: 7918993]
60. Walker M, Zhang XZ, Jiang W, Trinick J, White HD. Observation of transient disorder during myosin subfragment-1 binding to actin by stopped-flow fluorescence and millisecond time resolution electron cryomicroscopy: evidence that the start of the crossbridge power stroke in muscle has variable geometry. Proc Natl Acad Sci U S A. 1999; 96:465–470. [PubMed: 9892656]
61. Thomas DD, Ramachandran S, Roopnarine O, Hayden DW, Ostap EM. The mechanism of force generation in myosin: a disorder-to-order transition, coupled to internal structural changes. Biophys J. 1995; 68:135S–141S. [PubMed: 7787056]
62. Thomas DD, Prochniewicz E, Roopnarine O. Changes in actin and myosin structural dynamics due to their weak and strong interactions. Results Probl Cell Differ. 2002; 36:7–19. [PubMed: 11892285]
63. Svensson EC, Thomas DD. ATP induces microsecond rotational motions of myosin heads crosslinked to actin. Biophys J. 1986; 50:999–1002. [PubMed: 3790699]
64. Fajer PG, Fajer EA, Thomas DD. Myosin heads have a broad orientational distribution during isometric muscle contraction: time-resolved EPR studies using caged ATP. Proc Natl Acad Sci U S A. 1990; 87:5538–5542. [PubMed: 2164688]
65. Behrmann E, Muller M, Penczek PA, Mannherz HG, Manstein DJ, Raunser S. Structure of the rigor actin-tropomyosin-myosin complex. Cell. 2012; 150:327–338. [PubMed: 22817895]
66. Thomas DD, Seidel JC, Gergely J. Rotational dynamics of spin-labeled F-actin in the sub-millisecond time range. J Mol Biol. 1979; 132:257–273. [PubMed: 230351]
67. Miller MS, Palmer BM, Ruch S, Martin LA, Farman GP, Wang Y, Robbins J, Irving TC, Maughan DW. The essential light chain N-terminal extension alters force and fiber kinetics in mouse cardiac muscle. J Biol Chem. 2005; 280:34427–34434. [PubMed: 16085933]
68. Kazmierczak K, Xu Y, Jones M, Guzman G, Hernandez OM, Kerrick WG, Szczesna-Cordary D. The role of the N-terminus of the myosin essential light chain in cardiac muscle contraction. J Mol Biol. 2009; 387:706–725. [PubMed: 19361417]
69. Lowe DA, Surek JT, Thomas DD, Thompson LV. Electron paramagnetic resonance reveals age-related myosin structural changes in rat skeletal muscle fibers. Am J Physiol Cell Physiol. 2001; 280:C540–547. [PubMed: 11171573]
70. Lowe DA, Warren GL, Snow LM, Thompson LV, Thomas DD. Muscle activity and aging affect myosin structural distribution and force generation in rat fibers. J Appl Physiol. 2004; 96:498–506. [PubMed: 14514706]

71. Malik FI, Hartman JJ, Elias KA, Morgan BP, Rodriguez H, Brejc K, Anderson RL, Sueoka SH, Lee KH, Finer JT, Sakowicz R, Baliga R, Cox DR, Garard M, Godinez G, Kawas R, Kraynack E, Lenzi D, Lu PP, Muci A, Niu C, Qian X, Pierce DW, Pokrovskii M, Suehiro I, Sylvester S, Tochimoto T, Valdez C, Wang W, Katori T, Kass DA, Shen YT, Vatner SF, Morgans DJ. Cardiac myosin activation: a potential therapeutic approach for systolic heart failure. Science. 331:1439–1443. [PubMed: 21415352]

72. Haase H, Dobbernack G, Tunnemann G, Karczewski P, Cardoso C, Petzhold D, Schlegel WP, Lutter S, Pierschalek P, Behlke J, Morano I. Minigenes encoding N-terminal domains of human cardiac myosin light chain-1 improve heart function of transgenic rats. Faseb J. 2006; 20:865–873. [PubMed: 16675844]

73. Morano I, Ritter O, Bonz A, Timek T, Vahl CF, Michel G. Myosin light chain-actin interaction regulates cardiac contractility. Circ Res. 1995; 76:720–725. [PubMed: 7728988]

74. Rarick HM, Opgenorth TJ, von Geldern TW, Wu-Wong JR, Solaro RJ. An essential myosin light chain peptide induces supramaximal stimulation of cardiac myofibrillar ATPase activity. J Biol Chem. 1996; 271:27039–27043. [PubMed: 8900193]

75. Nieznanska H, Nieznanski K, Stepkowski D. The effects of the interaction of myosin essential light chain isoforms with actin in skeletal muscles. Acta Biochim Pol. 2002; 49:709–719. [PubMed: 12422241]

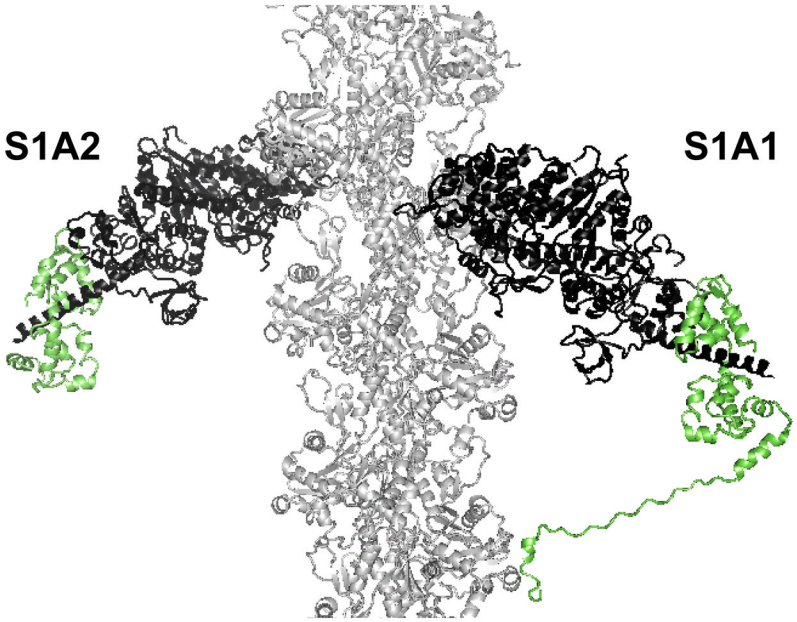

Figure 1.
Model of chymotryptic myosin fragments S1A1 and S1A2 (myosin heavy chain black, ELC green) bound strongly to actin (gray), with the N-terminal extension of the A1 ELC contacting subdomain 1 of a distant actin protomer. Adapted from Aydt et al.(25)

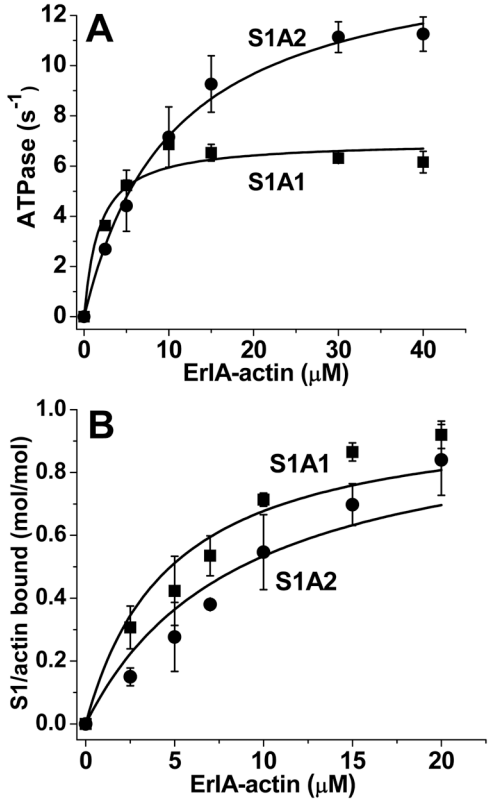

Figure 2.

(A) Actin-activated ATPase activity of S1 isoforms. (B) Binding of isoforms to actin in the presence of ATP. Both experiments were performed in Mg-F buffer plus 3 mM ATP. Curves were obtained from fits to Eq. 3 (A) and Eq. 2 (B), with results summarized in Table 1.

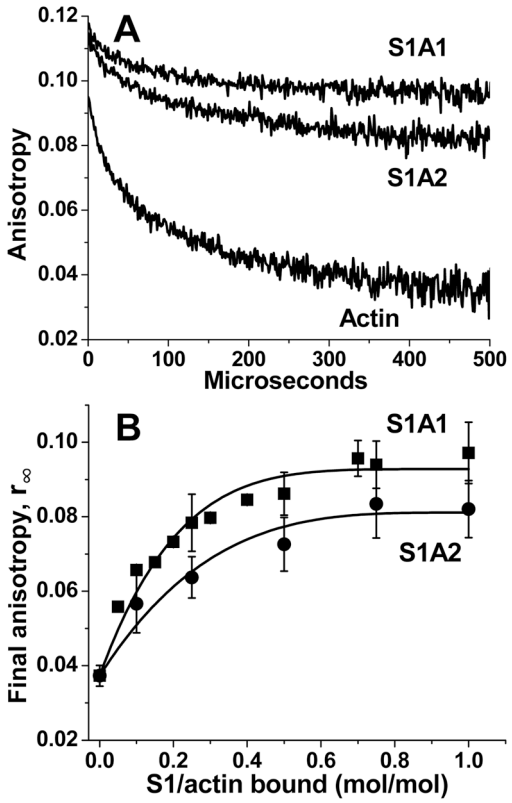

Figure 3.

The effect S1A1 or S1A2 (1.0 μM) on the final anisotropy of ErIA-actin (1.0 μM) in the absence of ATP. (A) TPA decays B. Final anisotropies at increasing fraction of actin protomers occupied by strongly bound S1, fitted to the linear lattice model (Eq. 1).

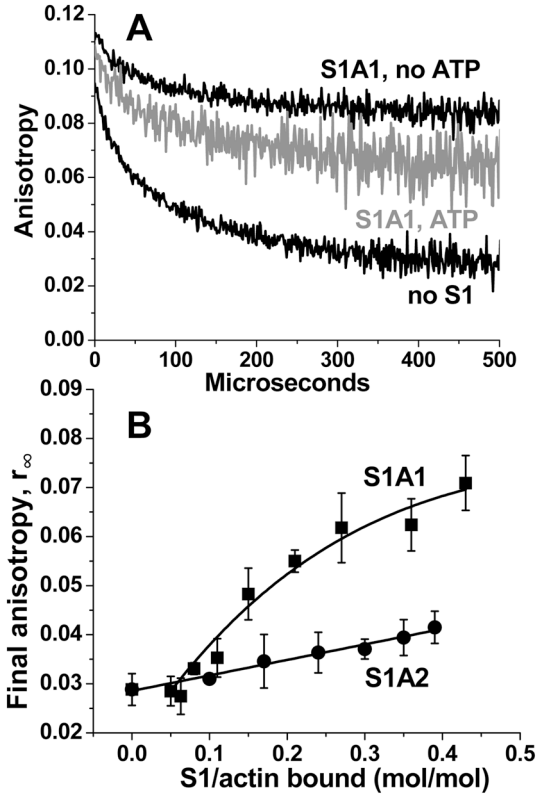

Figure 4.

The effect S1A1 and S1A2 on the actin dynamics in the presence of saturating ATP. (A) TPA decays of actin in the absence and presence of 3 mM ATP, at 0.4 moles S1A1 bound per mole of actin. (B) Final anisotropy as a function of the fraction of actin occupied by S1. S1A2 data were fitted by a straight line; S1A1 data were fitted by the linear lattice model starting at S1/actin bound = 0.05, giving N = 4.4±1.1 (Eq. 1).

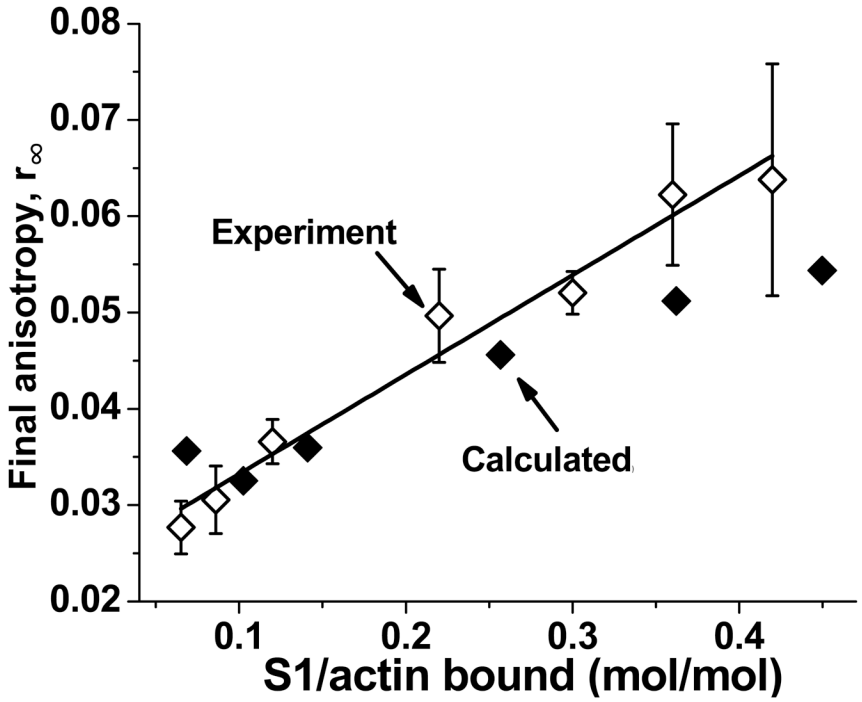

Figure 5.

The effect on final anisotropy of a 2:1 mixture of S1A1 and S1A2 (open diamonds) in the presence of saturating ATP, compared to a calculated (closed diamonds) linear combination of independently measured anisotropies, $r_\infty(\text{total}) = x_1 * r_\infty(\text{S1A1}) + x_2 * r_\infty(\text{S1A2})$. x_1 and x_2 are molar fractions of bound S1A1 and S1A2 calculated (Eq. 3) from the corresponding K_d values (Table 1), and $r_\infty(\text{S1A1})$ and $r_\infty(\text{S1A2})$ are final anisotropies obtained from the fits in Figure 4B.

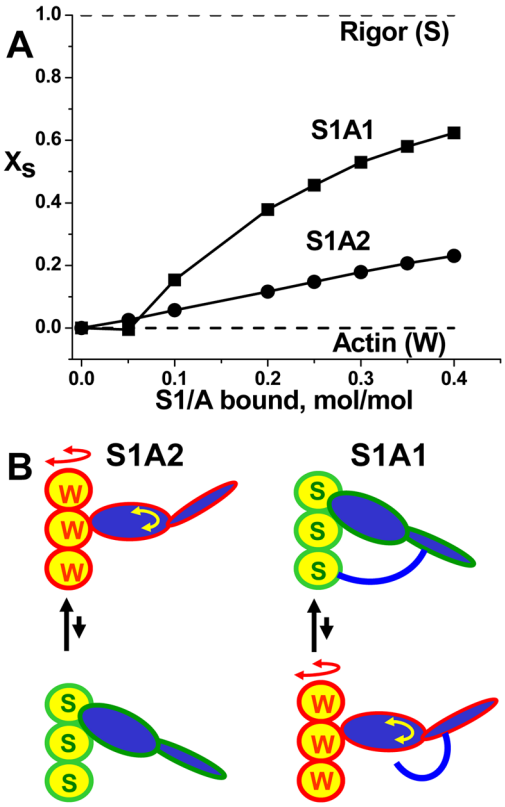

Figure 6.

A: Fraction of strongly bound structural states (X_S) of actin, as affected by isoenzymes in the presence of saturating ATP, calculated from Eq. 6. The final anisotropies r_∞ were obtained from (Figure 3) and (Figure 4), using (Eq. 1). B: Schematic illustration of the model, in which the distribution of *W* and S states depends strongly on the ELC isoform, and cooperativity occurs when one myosin head interacts with two actin protomers.

Table 1

Interaction of S1A1 and S1A2 with ErIA-actin in the presence of saturating ATP (from data in Figure 2)).

S1	V_{max} (s^{-1})	K_{ATPase} (μM)	Catalytic efficiency	K_d (μM)
	No KCl			
S1A1	7.0±0.4	1.8±0.6	3.9±0.8	4.8±0.7
S1A2	14.7±0.7	10.4±1.3	1.4±0.3	8.7±1.3
	25 mM KCl			
S1A1	8.0±0.7	12.5±2.7	0.64±0.12	10.6±1.0
S1A2	9.9±0.7	21.5±3.4	0.46±0.08	9.6±1.5

Assays performed in Mg-F buffer + 3 mM ATP without or with 25 mM KCl added. Catalytic efficiency = V_{max}/K_{ATPase}.($s^{-1}\mu M^{-1}$).